# Detecting gamma frequency neural activity using simultaneous multiband EEG-fMRI

Authors: Makoto Uji[a], Ross Wilson[a], Susan T. Francis[b], Stephen D. Mayhew[a], Karen J. Mullinger[a,b]

[a] Centre for Human Brain Health (CHBH), University of Birmingham, Birmingham, UK
[b] SPMIC, School of Physics and Astronomy, University of Nottingham, Nottingham, UK

## Synopsis (≤ 100 words)

We establish a methodology for optimal combination of simultaneous EEG recording with sparse multiband fMRI that preserves high resolution, whole brain fMRI coverage with broad-band EEG signal measurement uncorrupted by MR gradient artefacts. We demonstrate the ability of this approach to record gamma frequency (>50Hz) EEG signals, that are usually obscured during continuous fMRI data acquisition. In a novel application to a motor task we observe a positive correlation between gamma and BOLD responses, supporting and extending previous findings concerning the coupling between neural and haemodynamic measures of brain activity.

## Main Body (≤ 750 words)

### Purpose of Work

To assess the feasibility (safety and image quality) of simultaneously recording multiband fMRI with EEG and to show its potential for investigating relationships between EEG gamma activity and BOLD responses.

### Background

Multiband fMRI can provide shorter TR, increased brain coverage[1, 2] for a given TR, or shorter acquisition time in sparse fMRI which extends quiet periods for stimulus presentation. Sparse multiband fMRI has great potential for improving simultaneous EEG recordings where residual gradient artefacts typically obscure gamma frequency neural activity[3, 4]. However, due to the additional RF power of multiband excitation the safety of multiband EEG-fMRI acquisitions must be assessed [5] and the effect of EEG[6] and multiband[7] on EPI image quality.

### Methods and Analysis

MRplus EEG amplifiers and 64-channel EEG cap (Brain Products) were used with a 3T Philips Achieva MRI scanner and multiband acquisition (Gyrotools, Zurich), with MR-EEG clocks synchronised.

**Initial testing**

*Safety testing*

The EEG cap was connected to a conductive agar phantom. Fibre-optic thermometers (Luxtron) monitored the temperature of electrodes (ECG, Cz, TP7, FCz & TP8), cable bundle and the scanner bore throughout two 20-minute scans testing the upper bound of SAR: 1) GE-EPI (TR/TE=1000/40ms, slices=48, B1 RMS=1.09μT, SAR/head=22%); 2) PCASL-GE-EPI (TR/TE=3500/9.8ms, slices=32, B1 RMS=1.58μT, SAR/head=46%). Multiband factor 4 and SPIR fat suppression were used for both sequences.

*Image quality*

Data were recorded on 3 healthy-subjects during five different GE-EPI sequences: multiband factor=1-3 combined with slice acquisition spacing: equidistant or SPARSE (providing a quiet period with no gradients) all with TR/TE=3060/40ms, SENSE=2, slices=36, FA=79°, 41 volumes (see Fig. 2). A T1-weighted anatomical was acquired and grey matter segmented (FSL FAST) and to mask the fMRI data. Image quality was assessed by comparing grey matter temporal signal-to-noise ratio (tSNR).

**EEG-fMRI motor study**

*Paradigm*

A trial consisted of four abduction movements of the right-hand index finger, auditory cued (2.5Hz), performed within the MR quiet period of the SPARSE scan, with a 18s resting baseline interval. 8 subjects completed 4 runs of 30 trials inside the MR scanner.

*Data acquisition*

EEG-fMRI were acquired using a SPARSE GE-EPI scheme (TR/TE=3000/40ms, multiband factor=3, 33 slices (acquisition time=0.75s, quiet period=2.25s), voxels=3mm$^3$, 192 volumes, SAR/head<7%). Simultaneous EMG was recorded from right first dorsal interosseous. VCG recordings were acquired to aid pulse artefact correction. A T1-weighted anatomical image and electrode locations were recorded (Polhemus Fastrak) allowing EEG source localization.

*Data analysis*

*EEG*

Gradient and pulse artefacts were corrected, data downsampled (600Hz) and epoched from -16–2s relative to auditory cue onset (BrainVision Analyzer2). Trials contaminated with large artefacts/baseline EMG movements were removed. ICA was used to remove eye-blinks/movements (EEGLAB) and data were average referenced. A Linearly Constrained Minimum Variance beamformer was employed with individual boundary element head models (Fieldtrip[8]) to localise changes in gamma frequency (55–80Hz) power to abduction movements by creating pseudo Ŧ-statistic images [active: 0–1.8s and passive: -9.0 to -7.2s windows]. A broadband (1-120Hz) timecourse of neural activity was extracted

from the peak T-statistic location in the contralateral primary motor cortex (M1). Time-frequency spectrograms were calculated using a multitaper wavelet approach[4]. The mean gamma power per trial (0-1.5s after auditory cue onset) formed a regressor for fMRI analysis.

*fMRI*

fMRI data were motion corrected, spatially smoothed (5mm) and normalised to the MNI template (FSL). One subject was excluded due to stimulus-correlated motion. First-level GLM analysis employed 2 regressors: 1) boxcar abduction movement, 2) parametric modulation of single-trial gamma neuronal activity, convolved with the HRF. Data were grouped over runs and subjects using second- and third-level, fixed effects analysis.

## Results and Discussion

The GE-EPI showed the greatest heating effect in the ECG channel (~0.5° increase) with nominal heating in other channels (Fig 1). The higher SAR of the PCASL resulted in a greater heating effect (ECG ~0.9°). This heating was within safe limits but these data highlight the potential dangers with multiband sequences for EEG-fMRI where high SAR values can arise from the increased B1[9]. The variation in tSNR with multiband factor and slice spacing acquisition was relatively small (Fig 2). Multiband=3 with SPARSE spacing was chosen for the EEG-fMRI experiment, maximising MR quiet-period duration for EEG measurements.

Gamma EEG responses to finger abductions (Fig 3) were localised to contralateral M1. We observed both significant main-effect BOLD activation to the abduction movements (peak=-40,-28,56mm) and positive gamma-BOLD correlation in contralateral M1(peak=-30,-38,50mm) (Fig 4). This correlation was focal to the central sulcus and motor hand-knob, supporting a tight coupling of natural variability in BOLD and gamma task responses[4, 10]. These findings show the potential value of multiband EEG-fMRI for advanced study of brain function.
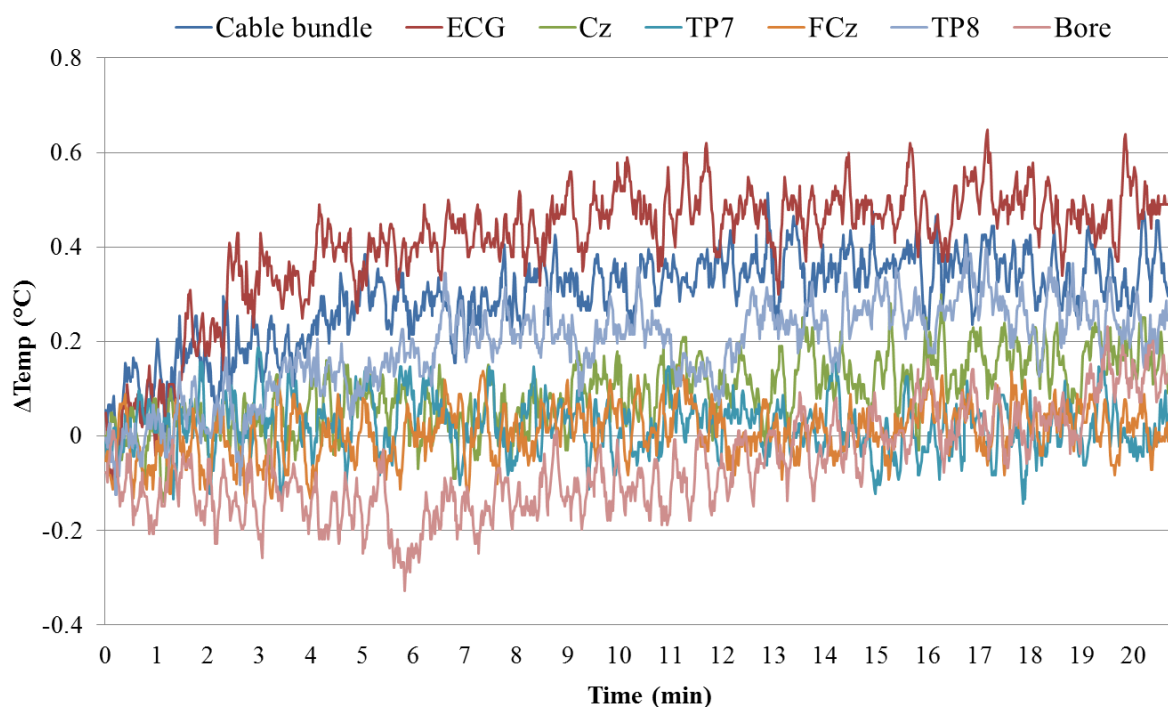
**Figure 1:** Temperature changes at EEG electrodes, cable bundle and a control location on the scanner bore during a 20-minute GE-EPI sequence scan in a Philips Achieva 3T MRI scanner. Temperature was calculated relative to a 5-minute baseline recording made before the scan.

| Multiband Factor | Slice acquisition spacing | tSNR |
|---|---|---|
| 1 | Equidistant | 74 ± 40 |
| 2 | Equidistant | 72 ± 39 |
| 2 | SPARSE | 67 ± 37 |
| 3 | Equidistant | 68 ± 37 |
| 3 | SPARSE | 74 ± 38 |

**Figure 2:** Mean tSNR (±SD) calculated over grey matter across 3 participants during five MR sequences: Multiband factors: 1-3; acquisition type = Equidistant or SPARSE. All other parameters were constant: TR/TE=3060/40ms, Sense=2, slices=36, FA=79°, Volumes=41.
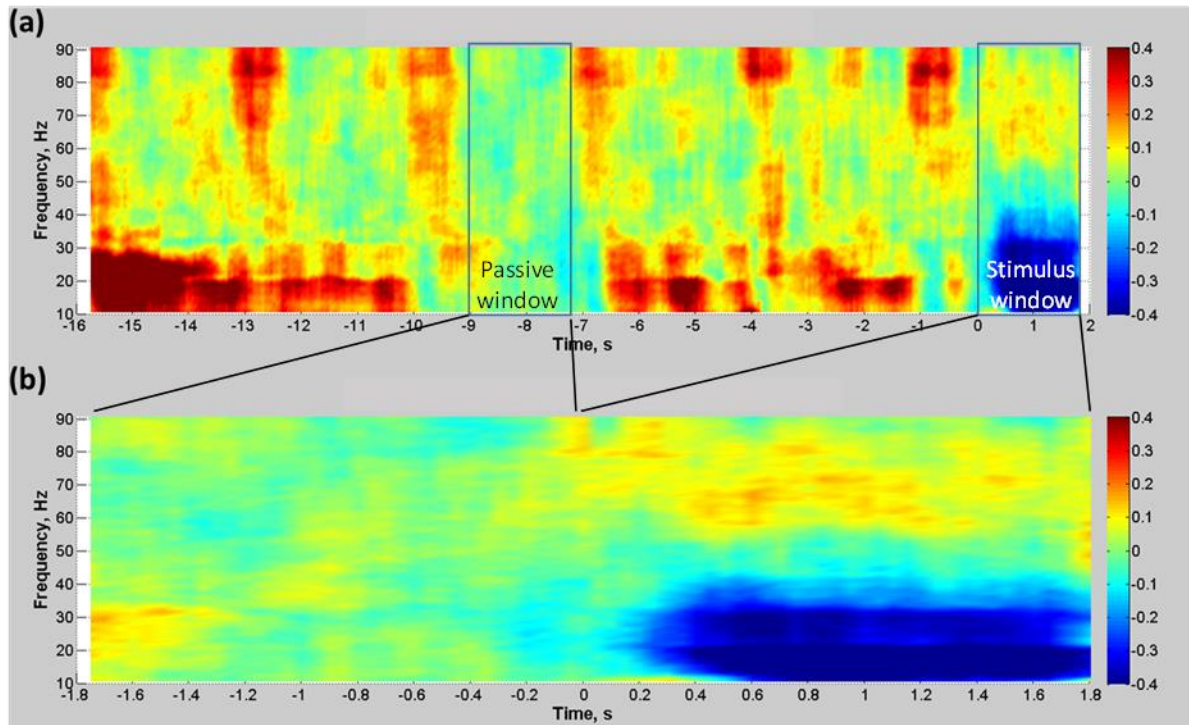
**Figure 3:** Mean time-frequency spectrograms from a representative subject demonstrating changes in the EEG signal power relative to the passive window (-9 to -7.2s). The passive window was located in an MR quiet period and before any anticipation of the stimulus. Time is displayed relative to the auditory cue onset. Spectrograms calculated with frequency resolution of 2.5Hz with spectral smoothing of ±10Hz [4]. **a)** 18s whole-trial duration, note the residual gradient artefacts during fMRI acquisition periods **b)** gamma and beta power responses during the active window (0 to 1.8s) where movement occurred, with the passive window data appended pre-stimulus for comparison.
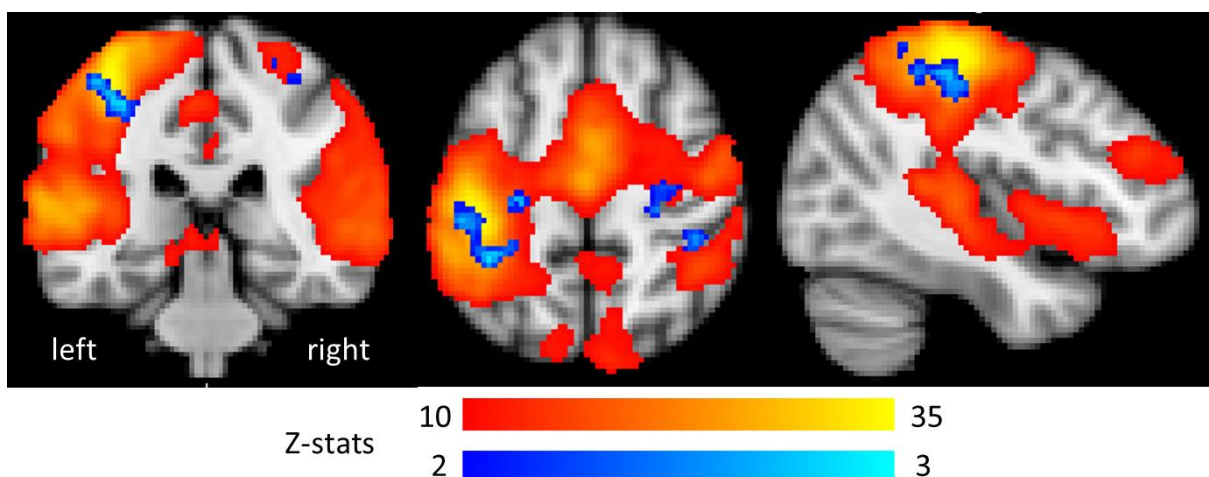


**Figure 4:** Group average (N=7) fMRI results. Main effect positive BOLD response to the right index finger abduction movements (red-yellow) and areas of positive correlation between single-trial EEG gamma and BOLD responses

(blue). Main effects are cluster corrected p<0.05, single-trial correlations p<0.001 uncorrected, masked with motor cortex.

## References

1. Feinberg, D.A., et al., *Multiplexed echo planar imaging for sub-second whole brain FMRI and fast diffusion imaging.* PLoS One, 2010. **5**(12): p. e15710.
2. Moeller, S., et al., *Multiband multislice GE-EPI at 7 tesla, with 16-fold acceleration using partial parallel imaging with application to high spatial and temporal whole-brain fMRI.* Magn Reson Med, 2010. **63**(5): p. 1144-53.
3. Mullinger, K.J. and R. Bowtell, *Combining EEG and FMRI.* Methods in molecular biology (Clifton, N.J.), 2011. **711**: p. 303-26.
4. Scheeringa, R., et al., *Neuronal Dynamics Underlying High- and Low-Frequency EEG Oscillations Contribute Independently to the Human BOLD Signal.* Neuron, 2011. **69**(3): p. 572-83.
5. Auerbach, E.J., et al., *Multiband accelerated spin-echo echo planar imaging with reduced peak RF power using time-shifted RF pulses.* Magn Reson Med, 2013. **69**(5): p. 1261-7.
6. Mullinger, K., et al., *Effects of simultaneous EEG recording on MRI data quality at 1.5, 3 and 7 tesla.* Int J Psychophysiol, 2008. **67**(3): p. 178-88.
7. Chen, L., et al., *Evaluation of highly accelerated simultaneous multi-slice EPI for fMRI.* Neuroimage, 2015. **104**: p. 452-9.
8. Oostenveld, R., et al., *FieldTrip: Open source software for advanced analysis of MEG, EEG, and invasive electrophysiological data.* Comput Intell Neurosci, 2011. **2011**: p. 156869.
9. Collins, C.M. and Z. Wang, *Calculation of radiofrequency electromagnetic fields and their effects in MRI of human subjects.* Magn Reson Med, 2011. **65**(5): p. 1470-82.
10. Logothetis, N.K., *The underpinnings of the BOLD functional magnetic resonance imaging signal.* J Neurosci, 2003. **23**(10): p. 3963-71.

## Acknowledgements